Ex-vivo micro-CT for the assessment of the structure of paraffin embedded coronary vessels before histology

Poster No.:	C-2257
Congress:	ECR 2012
Type:	Scientific Exhibit
Authors:	D. Panetta, C. Kusmic, G. Pelosi, F. Viglione, N. Belcari, A. Del Guerra, P. A. Salvadori; Pisa/IT
Keywords:	Cardiovascular system, CT-High Resolution, Instrumentation, Laboratory tests, Arteriosclerosis
DOI:	10.1594/ecr2012/C-2257

Purpose

Micro-CT is an established technique for high resolution three-dimensional (3D) imaging of small specimens [1]-[2]. Aim of the study was to demonstrate that absorption-based single low-energy micro-CT, using instrumentation available at laboratory level, can reliably separate different tissue components also in complex structures such as coronary arteries and the adjacent myocardium processed for standard histology after paraffin embedding.

The optimization of scan parameters, and in particular of the x-ray spectrum, is central for the purposes of this work. In fact, the "signal" (i.e., the image contrast) in absorption-based x-ray CT imaging depends on the relative differences of effective atomic number (Z_{eff}) and density (#) of adjacent structures. For most soft tissues, this difference is very small, thus many researchers are making efforts to study and implement alternative mechanism of contrast formation in CT, such as phase contrast [3]-[5]. The instrumentation required for phase contrast x-ray imaging is often restricted to highly specialized laboratories or synchrotron facilities. In this work, we optimized the scan settings of a small animal micro-CT scanner to study the capability of absorption-based high resolution x-ray CT for tissue differentiation in ex-vivo vascular samples.

It is known that, for a given material, both the linear attenuation coefficients (μ) and the image contrast (%C) with respect to a different background material, do increase with decreasing photon energies *E*, unless those materials present K- and L-edges that can alter the monotonic behavior of the μ(*E*) function in the energy range employed for acquisition. Fig. 1 on page 2 shows two different x-ray spectra from a W-anode source, together with the linear attenuation coefficients of some common organic materials [6]. Table 1 on page 3 reports the differences of theoretical CT contrasts between such materials, for the two spectra of Fig. 1 on page 2. The improvement at low energy is evident. For ex-vivo micro-CT studies, a lower limit for the mean energy <E> of the x-ray spectrum can be identified by taking into account the following issues:

- for each projection angle, a sufficient number of photons shall be gathered on the detector, to avoid unacceptable noise and reconstruction artifacts from photon starvation;
- the range of the x-ray fluences over the entire object cross-section must not exceed the dynamic range of the detector.

Images for this section:

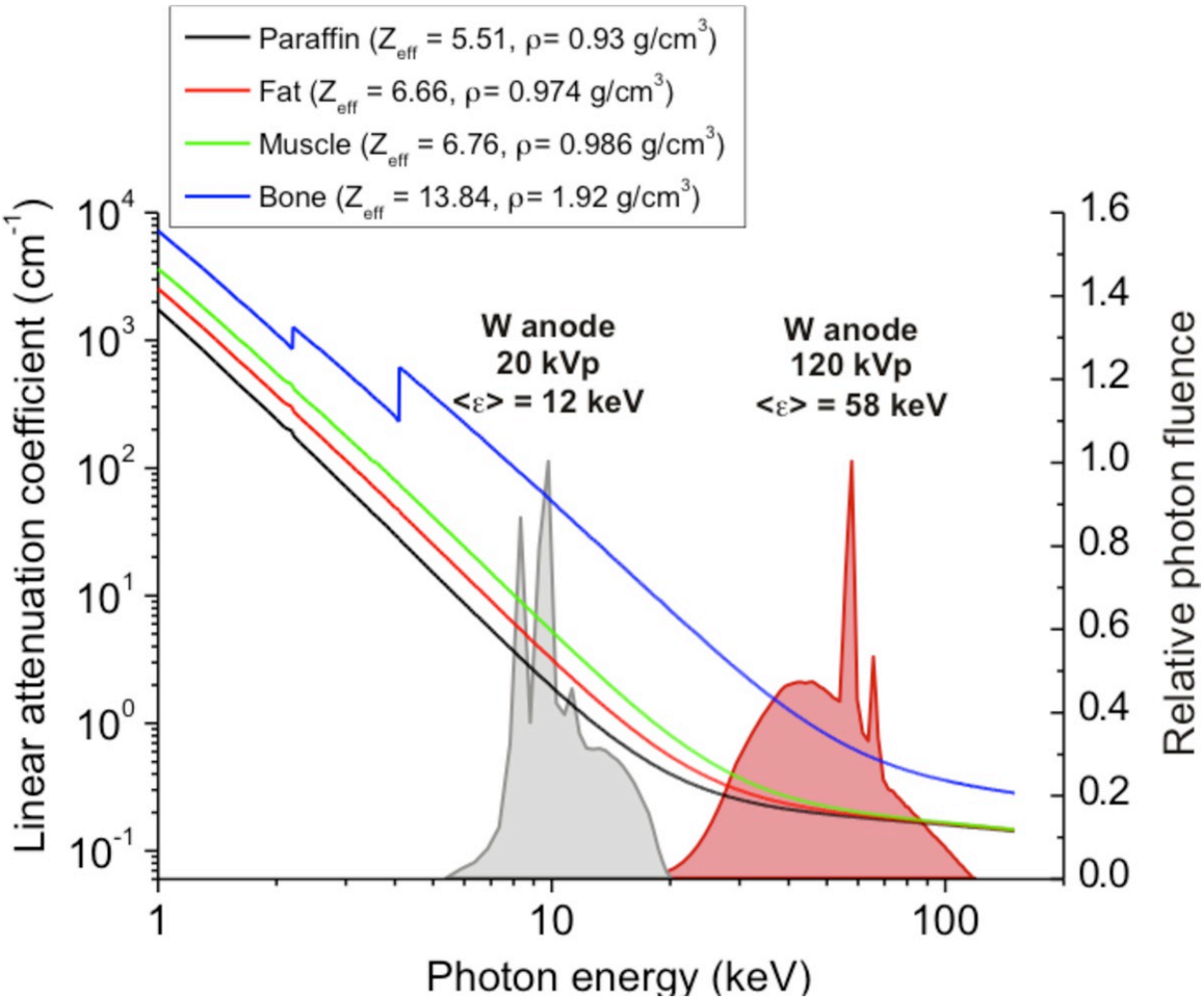

Fig. 1: Typical x-ray spectra from a tungsten anode for micro-CT (left, 20 kV) and clinical CT (right, 120 kV). In the graph it is also shown the energy dependence of the linear attenuation coefficients of various biological materials.

	20 kV (μCT – small samples)	120 kVp (Clinical CT – patient)
Bone vs. muscle	**945 %**	**220 %**
Muscle vs. fat	**63 %**	**5.6 %**
Muscle vs. paraffin	**163 %**	**10.8 %**
Fat vs. paraffin	**61 %**	**4.8 %**

Table 1: Theoretical percentage contrasts for various tissue/background pairs of biological interest, computed for the two spectra of Figure 1. The green rectangle highligths the relevant contrast values for micro-CT.

Methods and Materials

1) Micro-CT scanner

The Xalt scanner (X-ray AnimaL Tomograph, Fig. 2 on page 5) is a rotating gantry, cone-beam mCT for small animals [7]. It was built in the framework of a collaboration between the Institute of Clinical Physiology (IFC-CNR) and the Functional Imaging and Instrumentation Group (FIIG) of the Department of Physics "E. Fermi", University of Pisa.

The Xalt scanner allows to select the geometric magnification between scans to set a trade-off between spatial resolution and field-of-view (FoV). It is equipped with a W-anode microfocus X-ray source with accelerating potential in the range of 20-50 kV, and with a 10x5 cm^2 flat-panel CMOS detector with Gadox scintillator. For a single (non-helical) tomographic scan, the maximum transaxial FoV size is 80 mm in diameter for the 'Large FoV' (LF) setup, with an isotropic voxel size of 40 µm; the minimum voxel size is 18.4 µm in the 'High Resolution' (HR) setup. The minimum acquisition time is 43 s for fast, low-dose in-vivo scans, and can be as high as 4 hours for ex-vivo, low-contrast high resolution studies. Typical scan times are 2-10 min for in-vivo imaging of mice and rats at 40-80 µm resolution, and 10-90 min for ex-vivo scans of organs and biopsies at 18-40 µm resolution.

2) Samples and data acquisition

Data were obtained from an *ad-hoc* biological phantom and coronary specimens. The biological phantom was prepared composing and embedding together in paraffin two samples of rat fat and myocardium (previously fixed with formalin and dehydrated). This phantom was used to measure the image contrast of different tissues with respect to background. Real samples of explanted swine coronaries with native (diet induced) and accelerated (balloon hyperinflation) lesions, were processed in the same way and scanned with the same CT settings at various steps of histological processing. Then, reconstructed CT images were compared to histological findings (optical microscopy). The voxel size in the micro-CT images was in the range of 18-43 µm. The scan time varied in the range of 30-120 min.

Images for this section:

Fig. 2: The Xalt micro-CT scanner at the Molecular Imaging lab of IFC-CNR, during an animal study.

Results

1) Phantom studies

In phantom, the myocardium contrast vs. paraffin background varied from 40% at 20 kV to 29% at 50 kV. The average fat contrast vs. background was 2% at 20 kV, whereas it was actually indistinguishable from the background at 50 kV (Fig. 3 on page 7). All the contrasts in phantom appeared lower than those expected from theoretical computations, probably because of the sample processing that caused tissue shrinkage.

Following the phantom study, we fixed the x-ray beam quality at 20 kV, 0.1 mm Al, as the optimal setting for acquisitions on coronary samples.

2) Pig coronary sample (a): post balloon injury neointima

In one post-balloon injury coronary segment (Fig. 4 on page 8), intact vessel wall contrast was 25% greater than myocardium contrast; pericardium and neointima were clearly distinguished. The image quality was sufficient to perform threshold-based segmentation (Fig. 5 on page 8) that could allow quantitative measurement of volumes and tissue fractions within the selected Volume of Interest (VOI). In the current practice, this type of measurement can only be performed on multiple 2D consecutive histological sections.

3) Pig coronary sample (b): fatty streak

An early lesion (fatty streak, 0.25-0.5 mm thick), induced by high-fat hypercholesterolemic diet, that was present at the origin of the right coronary artery (RCA) could be identified at micro-CT as a subendothelial region with a density lower than that of tunica media and similar to periadventitial epicardial fat. Intimal thickness and intima-to-media thickness ratio of micro-CT and histological slices were comparable (Fig. 6 on page 9).

Alfa-smooth muscle actin (alfa-SMA) immunostain of smooth muscle cells was positive both in subendothelial areas within the fatty streak lesion itself as well as in the tunica media. The positivity (dark brown) of this cellular component paralleled that of CT density (red circle), whilst the prevalent foam-cells (lipid laden) cellular component had a much lower density (Fig. 7 on page 9).

Images for this section:

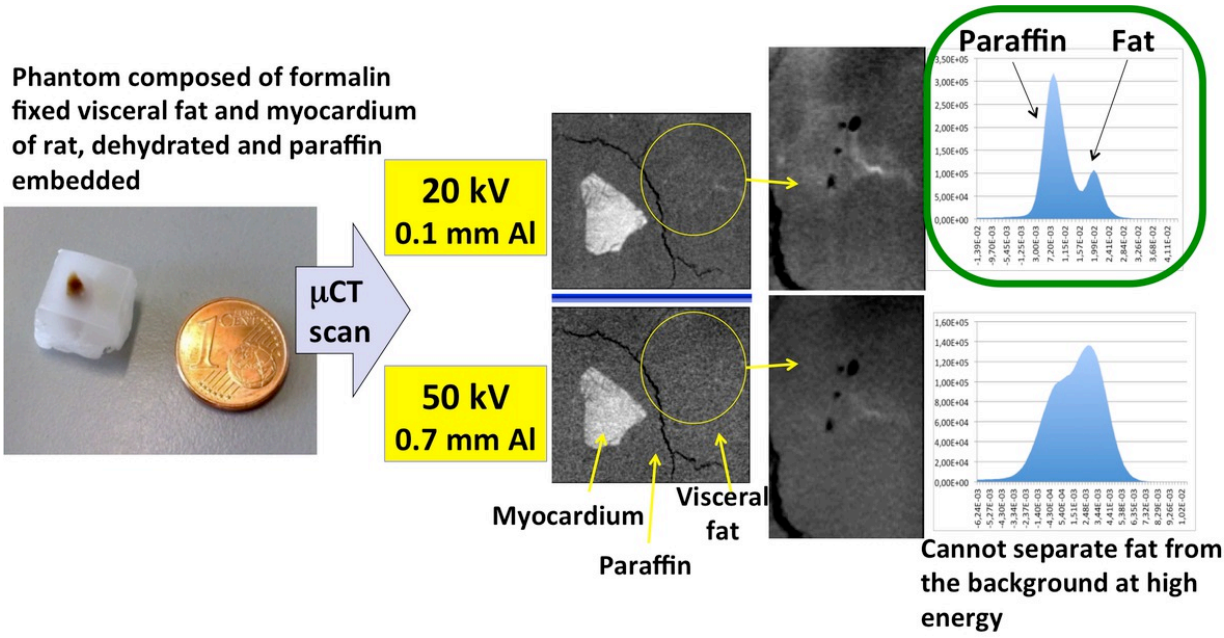

Fig. 3: In a paraffin background, the fat appeared visible only for the lowest energy settings available in the Xalt scanner (20 kV, 0.1 mm Al filtration). This is in disagreement with the theoretical results shown in Table 1, but it can be explained by considering the process of paraffin embedding that have modified the tissue structure and content of the adipose cells.

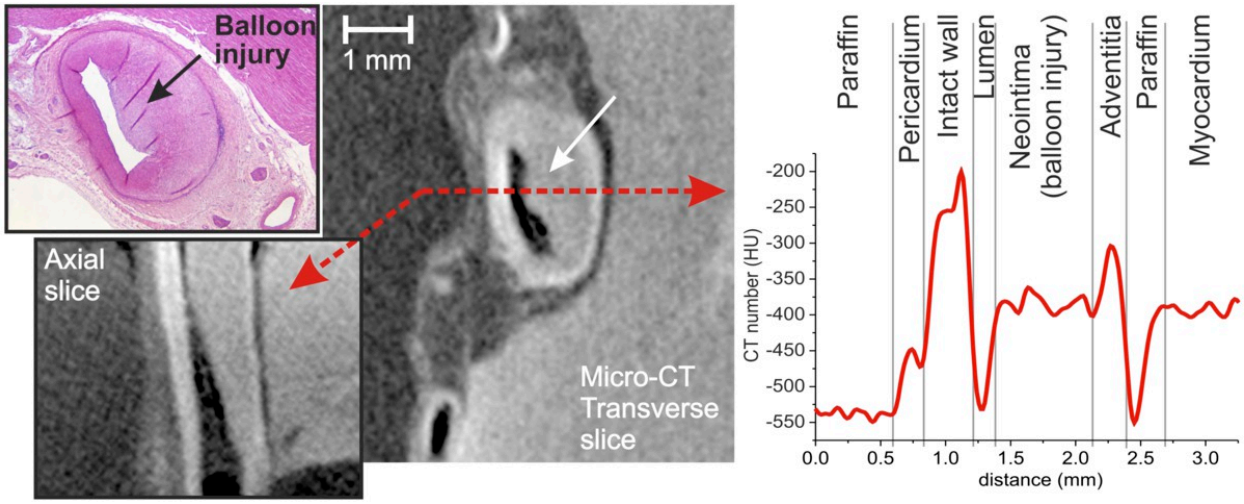

Fig. 4: Sample of pig LAD coronary artery with post balloon injury stenosis. The various layers of the arterial cross section are nicely separated and the shape of the neointima can be evaluated in 3D. Micro-CT (displayed in grayscale, 23 µm isotropic voxel) after paraffin embedding is superimposable to the corresponding microscopic image, allowing to fill the gap of information between the different histological plans of sectioning.

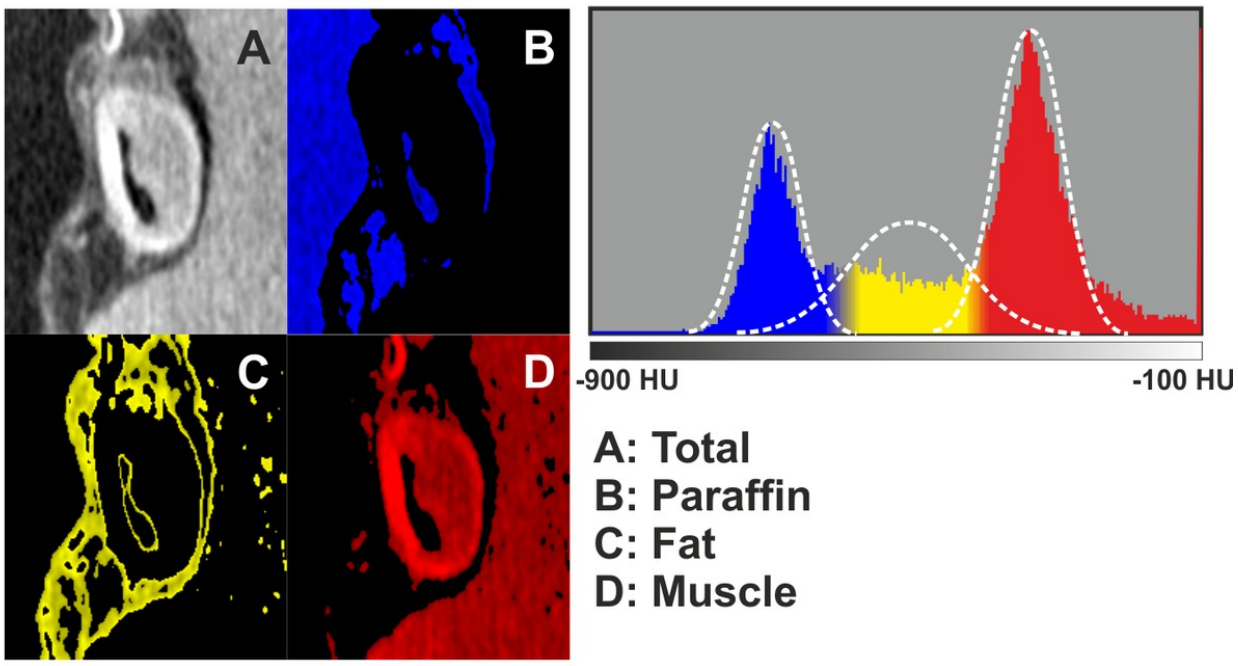

Fig. 5: Threshold-based segmentation of the image in Figure 5, showing the feasibility of tissue discrimination and volumetric measurement of different components.

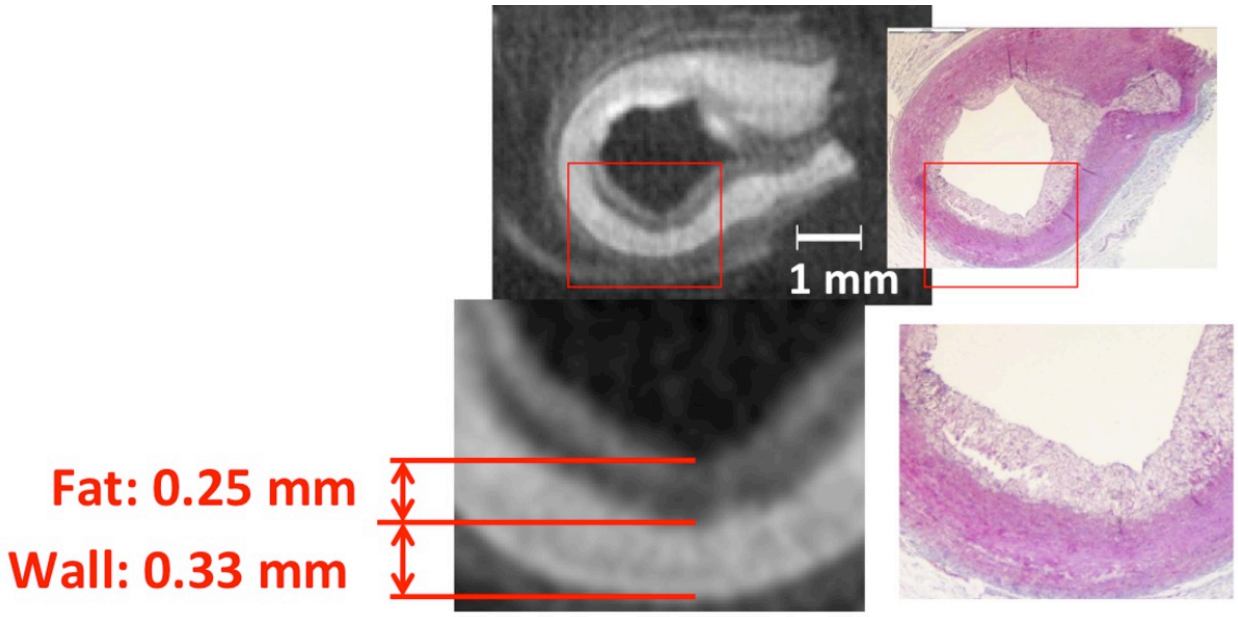

Fig. 6: High fat hypercholesterolemic diet induced lesion (fatty streak) at the origin of RCA. In micro-CT (left, voxel 23 µm), periadventitial fat and intimal atheroxantoma display similar gray level. At right, comparison with a neighboring histological cross-section (hematoxylin and eosin stain).

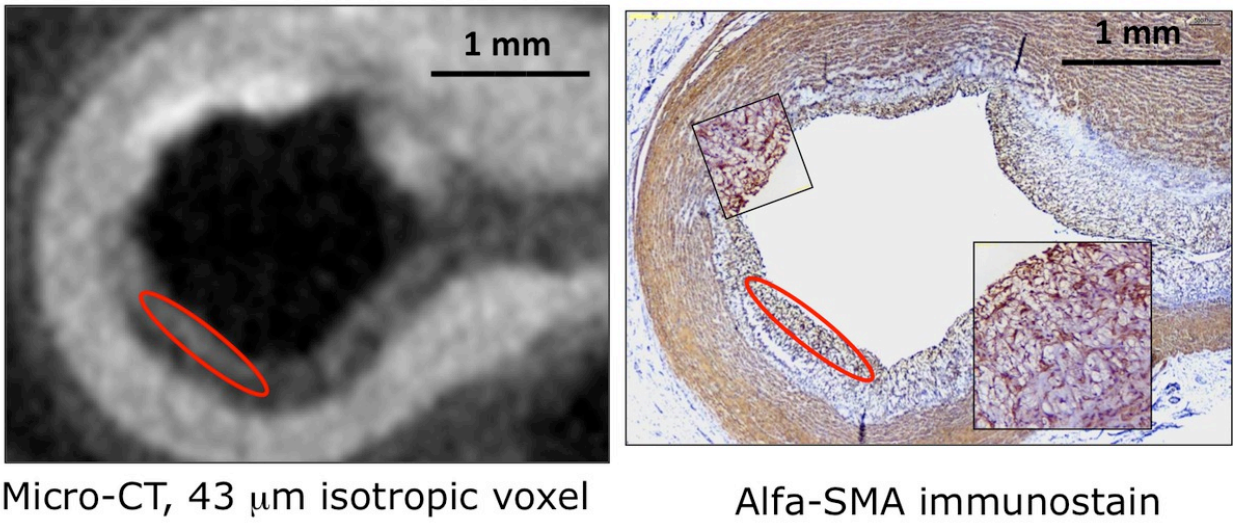

Fig. 7: Alfa-SMA positive immunostain (brown) of smooth muscle cells parallels micro-CT density within the lesion.

Conclusion

It is well established that x-ray CT is able to discriminate between tissues with highly different attenuation coefficients, such as blood/muscle vs. fat, bone, or iodinated contrast media. In this study we demonstrate that setting micro-CT at very low kV, compatibly with the specimen thickness and with the dynamic range of the x-ray detector, it is possible to adequately distinguish several normal and pathologic cellular components of the arterial wall, thus providing a useful complementary tool to histologic examination and pathologic diagnosis in standard paraffin-embedded samples. This type of imaging could represent a preliminary non-destructive screening of pathologic specimens aimed at identifying areas of interest both for experimental and diagnostic purpose.

References

[1] Paulus MJ, Gleason SS, Kennel SJ, Hunsicker PR, Johnson DK, High resolution X-ray computed tomography: an emerging tool for small animal cancer research. *Neoplasia* 2000; 2(1-2):62-70.

[2] Badea CT, Drangova M, Holdsworth DW, Johnson GA, In vivo small-animal imaging using micro-CT and digital subtraction angiography, *Phys. Med. Biol.* 53 (2008) R319-R350.

[3] Kaufmann R, Kottler C, Lohmann C, Revol V, Maake C, Luscher TF, Matter CM, Urban C, Phase contrast X-ray imaging - opportunities for applications in cardiology (#4779). Abstract presented at the ECR 2011 within the 'EIBIR presents: IMAGINE Workshop'.

[4] Endrizzi M, Carpinelli M, Delogu P, Oliva P, Golosio B, Gureyev TE, Bottigli U, Stefanini A, X-ray phase-contrast imaging with an Inverse Compton Scattering source, AIP Conf. Proc. 1266, 39 (2010); doi: 10.1063/1.3478194

[5] Beckmann F, Bonse U, Busch F, Günnewig O, X-Ray Microtomography (µCT) Using Phase Contrast for the Investigation of Organic Matter, *Journal of Computer Assisted Tomography*, (1997) 21 (4):539-553

[6] XMuDat, http://www-nds.iaea.org/reports/nds-195.htm

[7] Panetta D, Belcari N, Bartolomei A, Del Guerra A, Salvadori PA, Analysis of image sharpness reproducibility on a novel engineered micro-CT scanner with variable geometry and embedded recalibration software, *Physica Medica* (2011), doi:10.1016/ j.ejmp.2011.03.006 (in press)

Personal Information

D. Panetta, C. Kusmic, G. Pelosi, F. Viglione, P.A. Salvadori

CNR Institute of Clinical Physiology

Via G. Moruzzi, 1

I-56124 Pisa, ITALY

N. Belcari, A. Del Guerra

Dept. of Physics "E. Fermi"

University of Pisa

L.go B. Pontecorvo, 3

I-56100 Pisa, ITALY